THE IMPACT OF MICROWAVE ABSORBER AND RADOME GEOMETRIES ON GEODETIC MEASUREMENTS WITH GROUND-BASED GNSS ANTENNAS

T. Ning, G. Elgered, and J.M. Johansson

Department of Radio and Space Science, Chalmers University of Technology

Onsala Space Observatory, SE-439 92 Onsala, Sweden

ABSTRACT

We present results from an investigation on the impact of microwave absorber, i.e. ECCOSORB®, and radome geometries on geodetic measurements with ground-based Global Navigation Satellite System (GNSS) antennas. A 12 m baseline between two GNSS stations was used. One is an experimental station which can perform observations with various geometries of the Eccosorb and the radome. The other is the permanent ONSA station of the IGS network. Nine months of data from the baseline were analyzed with five different elevation cutoff angles from 5° to 25°. The 5.0 version of the GIPSY software, which provides antenna calibration and enables usage of the new GPS orbit and clock products from JPL, was used for the data processing. We found that the elevation-angle-dependent variations of the estimate of the vertical component of the relative site coordinates are significantly reduced by using the Eccosorb. The horizontal components are less affected. Two different configurations of the Eccosorb on the antenna give similar results. Small offsets were seen ($\sim 1-2$ mm) in the estimates of the vertical component of the baseline for 5°, 10°, and 15° solutions when the antenna is covered by a radome with a hemispheric top and a conical body. Using the Eccosorb also yields significant changes in the estimate of the atmospheric content of Integrated Water Vapour (IWV). The impact of using the radome affects the IWV less than 0.5 kg/m^2.

Key words: GNSS; GPS; Eccosorb; radome; atmospheric water vapour.

1. INTRODUCTION

After decades of continuous development, GNSS data from the Global Positioning System (GPS) have been used successfully in many applications. For example, continuously operating stations have significant advantages to determine the atmospheric content of Integrated Water Vapour (IWV) compared to other instruments, such as radiosondes and microwave radiometers [1]. Based on the highly precise orbit information and consistent Earth orientation parameters, the accuracy of horizontal position estimates from the GPS data is reaching the millimetre level [2], [3]. However, the characteristic of GNSS also makes it vulnerable to some errors. For example, in order to simultaneously track as many satellites as possible, the GNSS antennas have low directive gain with hemispheric coverage. This means that site-dependent systematic effects, i.e. scattering and multipath reflection from observations at low elevation angles cannot be neglected. Therefore, this type of error needs to be carefully investigated and mitigated to improve the performance of the GNSS technique.

The effects of multipath on geodetic estimates of site position obtained from GPS measurements have been shown in many studies, e.g. [4] and [5]. These found that the scattering from the reflecting structures within the near-field region (less than a few metres from the antenna), can produce relatively high errors (centimetre or greater) in the vertical coordinate estimates, but no significant effects in the horizontal parts. At a permanent GPS station, the top surface of the pillar, metal structures to support the antenna, and the edge of choke ring assembly of the antenna are possible sources for generating scattering.

To avoid the accumulation of snow and to protect from possible damages, many antennas of permanent GPS stations are equipped with a plastic cover (radome). Although radomes are designed to be transparent to the GPS signals, different shapes (mainly conical and hemispherical) could yield different impacts on the GPS measurement. Studies have been done to investigate such systematic errors [6] and [7]. They found that the hemispherical radome design is preferred to get high accuracy in the geodetic applications.

Here we address the influence of the effects of implementation of Eccosorb material and a hemispherical radome on the estimates of the relative site coordinates, and the IWV. In Section 2, we describe the construction of the experimental GPS station with a removable radome and microwave absorbers. In Section 3, the sessions of GPS

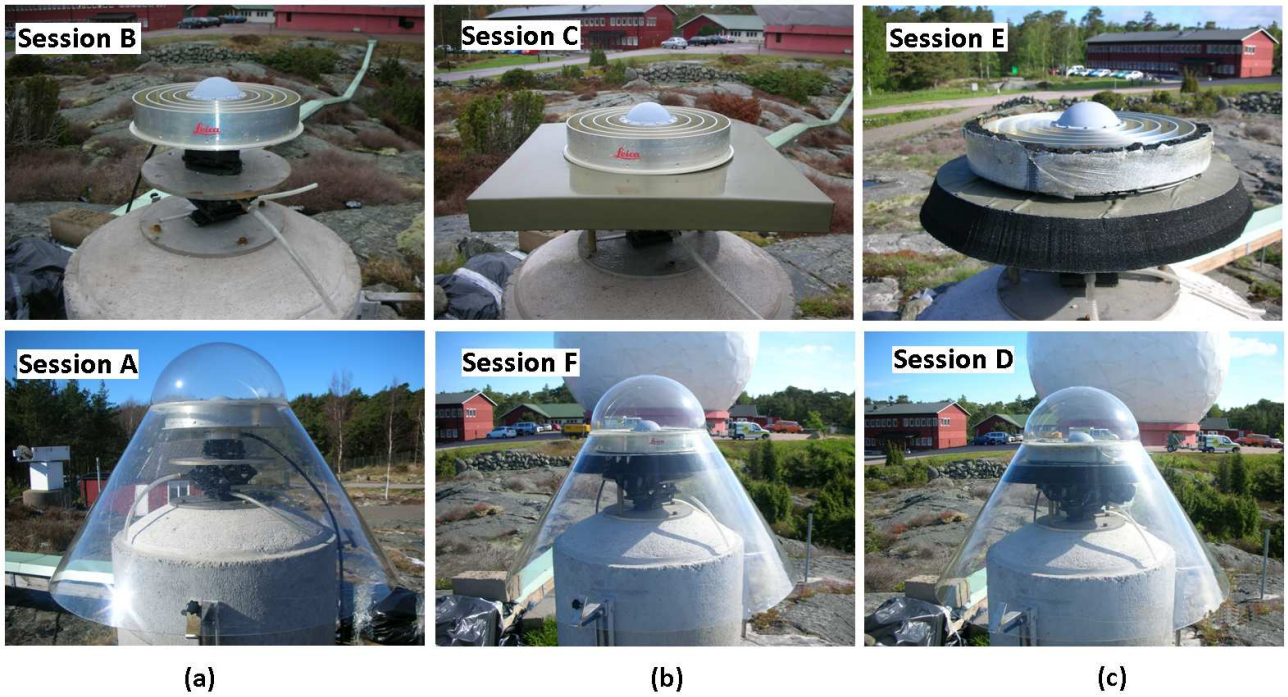

Figure 1. Photographs of the experimental station (ONTE) without (top) and with (bottom) radome having, (a) no Eccosorb, (b) the Eccosorb attached only below the antenna ground plane, and (c) the Eccosorb attached both below and around the antenna. The different sessions are further described in Section 3 and Table 1.

Figure 2. Photograph of the established baseline between two GPS stations (ONTE and ONSA are in the left and middle background, respectively), and the water vapour radiometer (WVR) is in the right background.

Figure 3. Photographs of the permanently operating GPS station (ONSA) in the IGS tracking newwork with a hemispheric radome and an Eccosorb sheet. This configuration was identical for all data acquisition.

observations with different configurations of the experimental station are presented. The way of processing the acquired GPS data is also discussed. Section 4 presents results and discussions regarding the differences of using two versions of the GIPSY software for data processing, impacts on the relative coordinates of a baseline and the IWV for different geometries with the Eccosorb and the radome. The conclusions follow in Section 5.

2. EXPERIMENTAL SETUP

During the autumn of 2005, an experimental pillar was constructed for flexible mounting of GNSS antennas over a reference marker, namely ONTE, at the Onsala Space Observatory. A Leica AT504GG antenna was mounted on a circular concrete pillar with a height of 1 m. A 3-dimensional positioning adjustment was mounted below the antenna which therefore can be moved in different directions with respect to the radome and the pillar (see Figure 1(a)). The continuously operating IGS station (ONSA) is 12 m (see Figure 2) away from the ONTE an-

Table 1. The sessions of observations at the experimental GPS station (ONTE)

Sessions	Configuration of the antenna	Start	End	Days of data recording	Figure
A1	With radome, no Eccosorb	2008/10/15	2008/11/17	32	1a (bottom)
B1	No radome, no Eccosorb	2008/11/17	2008/12/23	26	1a (top)
C	No radome, with Eccosorb put under the antenna only	2008/12/23	2009/03/19	63	1b (top)
B2	No radome, no Eccosorb	2009/03/19	2009/04/02	13	1a (top)
A2	With radome, no Eccosorb	2009/04/02	2009/04/14	7	1a (bottom)
D	With radome, with Eccosorb put under and around the antenna	2009/04/30	2009/05/18	17	1c (bottom)
E	No radome, with Eccosorb put under and around the antenna	2009/05/26	2009/06/08	12	1c (top)
F	With radome, with Eccosorb put under the antenna only	2009/06/08	2009/06/22	12	1b (bottom)

tenna. The ONSA antenna (AOAD/M_B) is centered in a choke ring assembly on the top of a 1 m high concrete pillar (see Figure 3). The Eccosorb is attached around the edge of the choke ring and a hemispheric radome is used to cover the antenna. During the experiment, the ONTE antenna is always fixed in the centre of the pillar. When the radome is put on the antenna, it is always in the centre with respect to the pillar. The type of the Eccosorb used is the Eccosorb AN-W 77 with standard size 61 cm x 61 cm x 5.7 cm. It is designed to reflect less than -20 dB of normal incident energy with frequencies above 1.2 GHz and is therefore suited for the GPS frequencies (1.23 GHz and 1.58 GHz). An Eccosorb sheet was also shaped to fit into the radome (Session F), and was put below the antenna to block the scattering from the top surface of the pillar and the metal plate to support the antenna. An Eccosorb ring was produced to cover the whole circumcentre of the choke ring to reduce the scattering effects from this part (Sessions D and E). All measurements of a certain set-up of the Eccosorb were performed twice (with and without radome). A water vapour radiometer (WVR) was also used. The WVR measures the sky emission at two frequencies, 21.0 and 31.4 GHz. The amount of water vapour along the direction of the observation can be inferred from the measured brightness temperatures. Elgered and Jarlemark [8] give a detailed description of the WVR and the corresponding data analysis. The WVR is mounted 10 m from the site of ONSA, and at approximately the same height (within 0.5 m). The analysis of the WVR is not yet carried out, but we foresee that comparisons to the GPS results will be included in the conference presentation two months from today.

3. GPS DATA ACQUISITIONS AND ANALYSIS

We first made observations with and without the radome on the antenna for the two continuous sessions (A1 and B1) where no Eccosorb was used. In Session C, the Eccsorb sheet was attached below the antenna only without the use of the radome. The same set-up of the Eccosorb, but covered by the radome was used in Session F. Two sessions (D and E) were performed with Eccosorb put both below and around the antenna, with and without the use of the radome. To investigate the reproducibility of the results, identical configurations from the previous sessions were set up, i.e. the sessions of A2 and B2. Table 1 specifies the details in the configurations of the experimental antenna in each session of observations. For some days, when we changed the configuration of the experiment or with data missing due to the computer problems, data were taken out from the processing. Therefore, the numbers given in the column of days of data recording are the days which have been put into the data analysis. Also it should be noted that there are no changes on the IGS station (ONSA) during the whole experiment.

The acquired GPS data were analyzed by the GIPSY-OASIS II software developed by the Jet Propulsion Laboratory (JPL) [9], with a processing strategy called Precise Point Positioning (PPP) [10]. Instead of using differential methods to eliminate the clock parameters in other GPS software packages, GIPSY estimates all relevant error signals based on a Kalman filtering technique known as a Square Root Information Filter (SRIF). Final precise orbits and consistent Earth orientation parameters, provided by IGS are used with the latency of about 13 days. The accuracy of the final IGS orbits is approximately 10 cm or better [11]. The zenith wet delay, the values of the propagation delay due to water vapour, were estimated as a radome walk process 1 cm/$\sqrt{\mathrm{h}}$ and updated every 300 s. A model presented in [12] depending on the latitude of the site and the day of the year was used to convert the zenith wet delay into the IWV. An ocean tide loading model was used in the processing [13].

To achieve centimetre or better accuracy of vertical coordinate estimates, the phase calibrations of GNSS antennas are necessary [14]. During 2008, the JPL has released a new version of GIPSY that provides increased support for antenna calibrations and enables usage of the

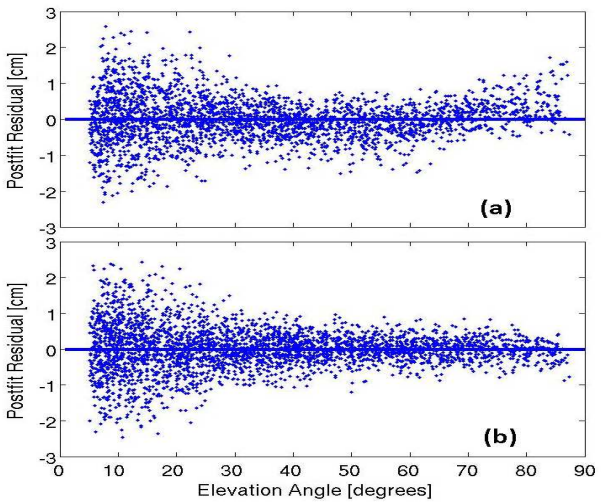

Figure 4. Postfit LC (ionospheric free linear combination) phase residuals from the experimental site (ONTE) for all satellites obtained from the process using (a) the old version of GIPSY (V4.0) and (b) the new version of GIPSY (V5.0). The data set were acquired on March 3rd, 2009 (Session C).

new consistent GPS orbit and clock products from JPL. In this work, we used both versions of GIPSY to process the data. However, the results from the old version of GIPSY (V 4.0) are only used to make comparisons to investigate the impacts of antenna corrections and usage of new orbit/clock products. The results related to the impact of Eccosorb and the radome are obtained from the new version of GIPSY (V 5.0), since we want to separate the antenna effects from those due to the electromagnetic environment.

4. RESULTS AND DISCUSSIONS

4.1. Impacts of Antenna Corrections

It is important to note that the multipath effects are mixed with the errors associated with the antenna itself, which are due to the antenna phase centre variations. This type of elevation angle dependent error is clearly seen in Figure 4(a) with the postfit LC phase residuals obtained from the old version of GIPSY (V4.0). To get better accuracy, this error must be corrected by implementing absolute phase calibration of the antenna which has to be done in the ideal environment, e.g. anechoic chambers [15]. The new version of GIPSY (V5.0) includes calibrations for most of the existing types of GNSS antennas. A significant part of the variations are removed (see Figure 4(b)) when processing with GIPSY V5.0. Figure 5 shows comparisons of the mean postfit LC phase residulas for the Session B, C, and E obtained by two versions of the GIPSY. The RMS scatter(standard deviatin around zero) of the residuals is given numerically.

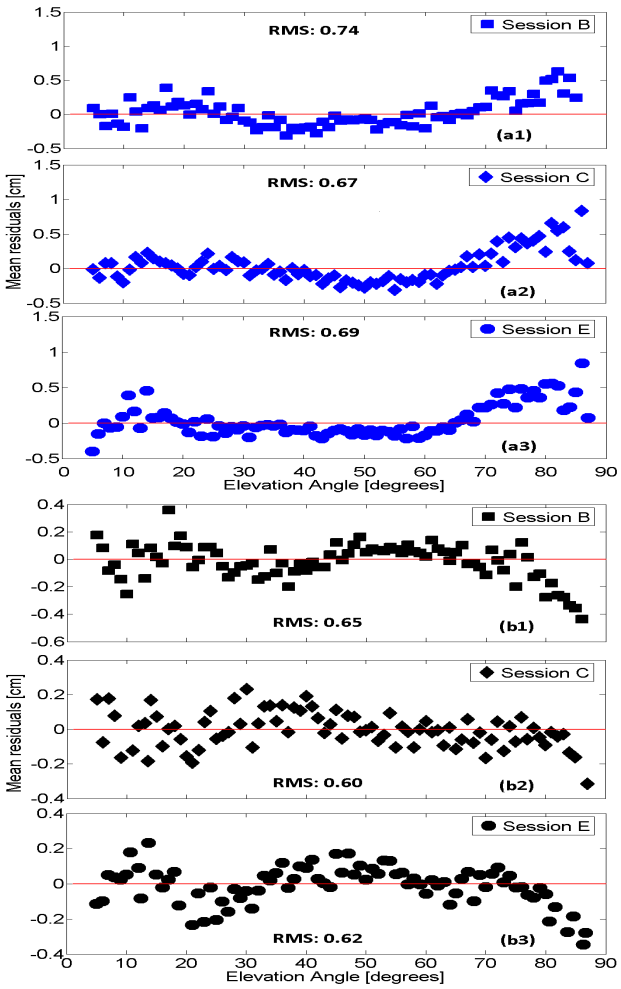

Figure 5. Comparisons of the mean Postfit LC phase residuals from the experimental site (ONTE) for all satellites obtained from the processing using (a) the old version of GIPSY (V4.0) and (b) the new version of GIPSY (V5.0) for the Sessions B, C, and E.

It is clear that for the same session the RMS from the GIPSY V4.0 are always bigger than the ones from the GIPSY V5.0. The results also show that implementation of the Eccosorb improves the residuals, no matter which version of GIPSY was used. The 0.07 and 0.05 cm decreases in RMS from the GIPSY V4.0 and V5.0 respectively are observed when the Eccosorb was only put under the antenna (see Figure 5 (a2) and (b2)). Those numbers change to 0.05 and 0.03 cm when the Eccosorb was put both under and around the antenna (see Figure 5 (a3) and (b3)).

4.2. Impacts on Estimates of Relative Site Positions

Figure 6 shows the elevation angle dependence of the RMS repeatabilities in the east, north, and vertical components of the baseline. All results are obtained without using the radome except the one shown in

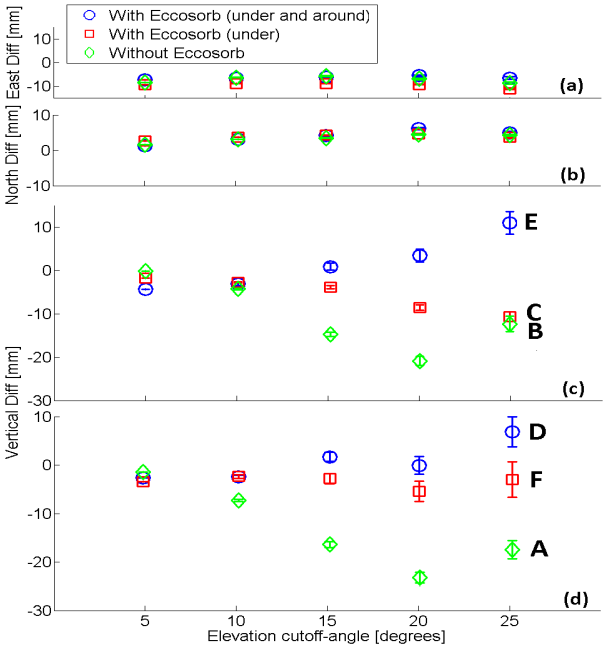

Figure 6. The elevation angle dependent variations on the estimated (a) east, (b) north, (c) vertical components of the baseline without radome (Sessions B, C, E) and (d) the vertical component with radome (Sessions A, D, F). The results were obtained without Eccosorb (diamonds, A and B), with Eccosorb put under only (squares, C and F), and put under and around (circles, D and E), the antenna. The error bars are the uncertainties of the differences, which are explained in the text, relative to the 5° solution.

Figure 6(d). Plotted data points are relative to the value from the 5° cutoff angle solution of the Session B1+B2 (no use of the Eccosorb and the radome). The error bars are the statistical standard deviations of the differences explained in [16]. The results demonstrate significant deviations (the maximum is 20 mm between the 5° and the 20° solution) in the vertical component if there is no Eccosorb attached to the antenna (see Figure 6(c) and (d)). The horizontal components have no clear impacts (see Figure 6(a) and (b)). The results also show that the implementation of the Eccosorb significantly, but not completely, removes the variations with the elevation angle. This can be seen in Figure 7 where the daily estimates of the vertical component of the baseline from different configurations of the Eccosorb for five different elevation cutoff angles are given. The error bars presenting the formal error of the estimate were omitted to increase the visibility. They are on average 2.8, 3.8, 5.5, 8.3 and 12.2 mm for the 5°, 10°, 15°, 20° and 25° solution, respectively. The mean offsets were obtained from different elevation cutoff angle solutions relative to those from the 15° solutions are given numerically in Figure 7, along with the 1-σ uncertainty of the offset. The uncertainty was calculated by dividing the weighted mean of the formal errors of the estimates by the square root of the number of days. As shown in Figure 7(a), the offsets of the 5° and the 10° solutions relative to the 15° solutions are -15 ± 1.18 and -10.8 ± 1.28 mm

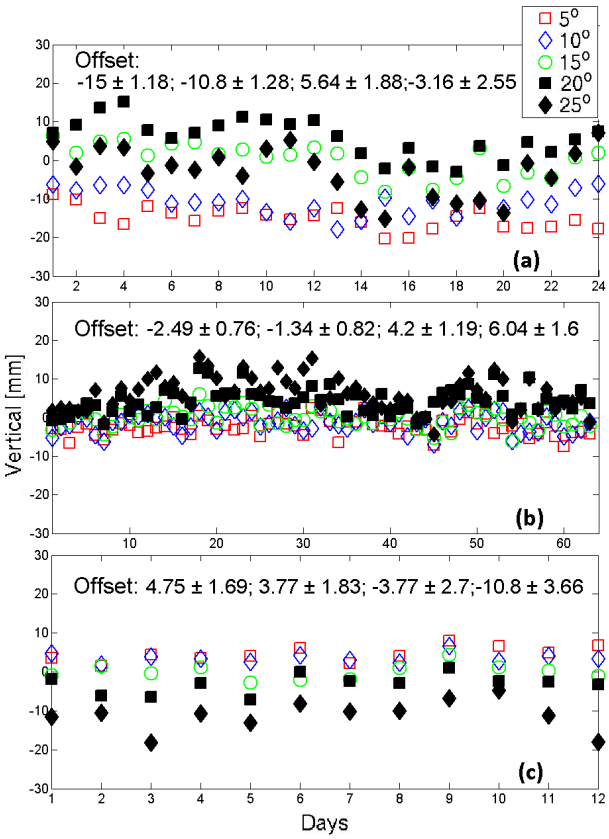

Figure 7. Daily estimates of the vertical component of the baseline for five different elevation cutoff angles, namely 5°, 10°, 15°, 20° and 25° from (a) no Eccosorb (Session B), (b) Eccosorb put only under the antenna (Session C), and (c) Eccosorb put both under and around the antenna (Session E).

when no Eccosorb was used. The offsets are decreased around 80% to -2.49 ± 0.76 and -1.34 ± 0.82 mm for Session C where the Eccosorb was only put under the antenna (see Figure 7(b)). Approximately 65% changes are seen (4.75 ± 1.69 and 3.77 ± 1.83 mm) when the Eccosorb was put both under and around the antenna (see Figure 7(c)). Results from the offsets between 20° and the 15° solutions show no large difference (5.64 ± 1.88, 4.2 ± 1.19, and -3.77 ± 2.7 mm) for the three sessions. There is however one exception in the results between the 25° and the 15° solutions, where the offsets (-10.8 mm and 6.04 mm) with Eccosorb are larger than the one (-3.16 mm) without using the Eccosorb. However, this exception is not seen in the results obtained from the sessions where the radome was on the antenna (see Figure 6(d)). This is possibly caused by the relative smaller data sets from Session E and F (12 days). Therefore, no significant difference (>3-σ) are here evident between the two different configurations of the Eccosorb.

To investigate the impacts of the usage of the radome with the hemispheric top and the conical body, we made com-

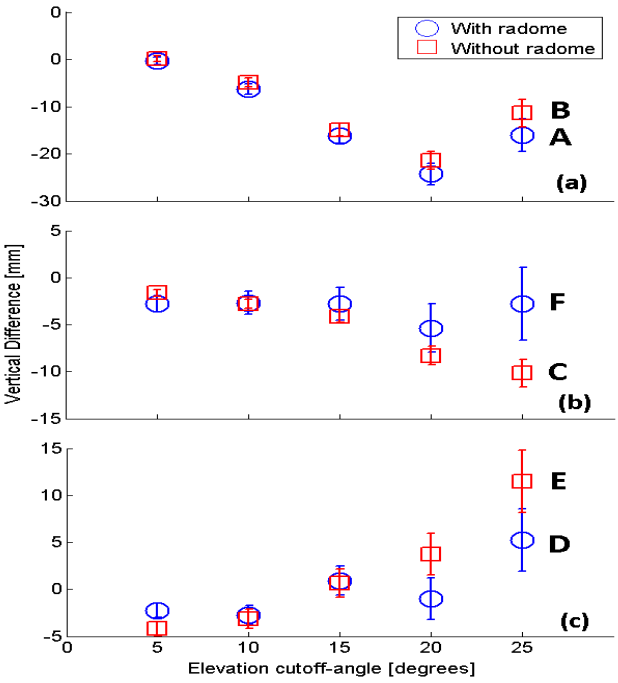

Figure 8. Comparisons on the estimated vertical component of the baseline obtained with and without the radome. The error bars are the 1-σ uncertainty of estimates calculated at the same way as the ones given for Figure 7. The results were obtained from the sessions where no Eccosorb attached to the antenna (a), the Eccosorb only was put under the antenna (b), and the Eccosorb was put both under and around the antenna (c).

parisons on the estimates of the vertical component of the baseline obtained from the sessions with and without using the radome. The results of the comparisons are given in Figure 8 plotted in the same way in Figure 6. The results show that the effect of the radome is approximately constant and have much less elevation dependence. Small offsets ($\sim$1$-$2 mm) are introduced by the radome on the estimated vertical component for the 5°, 10°and 15° solutions. Relatively large offsets are seen from the results for the higher elevation cutoff angle solutions, but with higher uncertainties (see Figure 8(c) and (d)). The maximums offset are around 6.1 and 6.7 mm along with the uncertainties of 4.7 and 4.3 mm, respectively for the 25° solutions. Therefore, relative to the uncertainties, the results show no significant influence ($>$3-σ) on the estimated vertical component of the baseline when the radome was used.

4.3. Impacts on Estimates of the IWV

Figure 9 shows the time series of the IWV for the nine months of October, 2008 to June, 2009, estimated from the two GPS stations. The top curve shows the results obtained from the IGS station (ONSA) with an offset of 20 kg/m^2 of the ONSA data in order to improve the visual comparison. The results show that the estimated IWVs

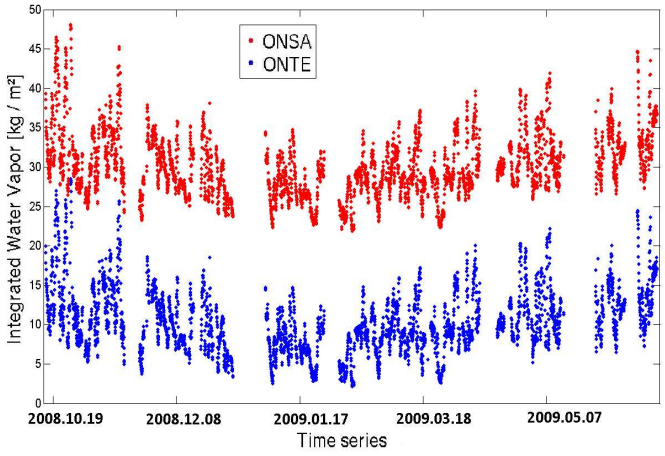

Figure 9. A comparison of the IWV estimates from two GPS stations and the WVR. The ONSA data has been offset by 20 kg/m^2.

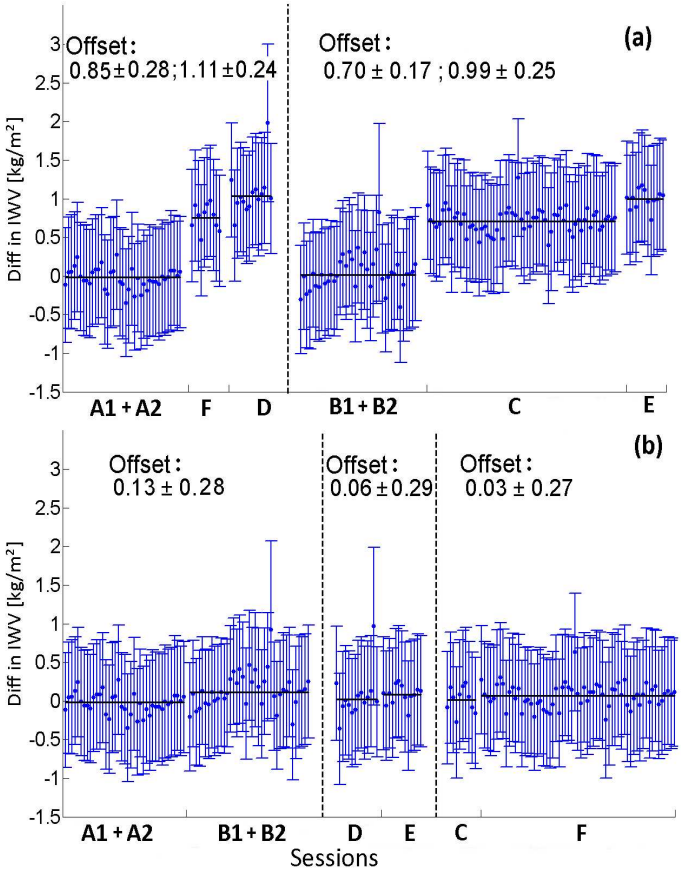

Figure 10. Daily statistics of the IWV for the comparison between two stations. The dots indicate the daily difference and the error bars represent the standard deviation of the difference of the mean for each day. (a) gives impacts from the installations of the Eccosorb and (b) shows effects from the usage of the radome. The mean value of each session is shown by solid lines. The estimates are obtained using an elevation cutoff angle of 15°.

are highly correlated to each other.

One example of the detailed statistics of the IWV obtained from the two GPS stations are given in Figure 10, where the daily mean differences of the IWV from the 15° solution are shown. The offsets in the difference, relative to the those estimated without using Eccosorb (Session A1+A2 and B1+B2, respectively), are given numerically, along with the 1-σ uncertainty of the offset. The calculation of the uncertainty is the same as the one we explained above (see Section 4.2). The results from Figure 10(a) show that for the sessions of A1+A2, F, and D, significant offsets in 0.85 $\pm$ 0.28 and 1.11 $\pm$ 0.24 kg/m^2 were caused with the implementation of the Eccosorb. The offsets change slightly to 0.70 $\pm$ 0.17 and 0.99 $\pm$ 0.25 kg/m^2 for the sessions with repeated configurations of the Eccosorb, but with the radome on the antenna (B1+B2, C, and E). The difference in results from sessions with the two types of the installations of the Eccosorb are negligible ($\sim$1-σ) in 0.26 and 0.29 kg/m^2, respectively. Figure 10(b) focus on the offset in the difference of the IWV caused by the radome. The offsets are 0.13 $\pm$ 0.28 kg/m^2 between the sessions of A1+A2 and B1+B2, 0.06 $\pm$ 0.29 kg/m^2 (D and E), and 0.03 $\pm$ 0.27 kg/m^2 (C and F). We therefore conclude that the results show no significant influence on the estimated IWV from the usage of the radome.

Figure 11 and Figure 12 show the impact of the implementation of the Eccosorb and the radome on the estimated IWV (c.f. Figure 6 and Figure 8 for the vertical component) for different cutoff angles. These results are highly correlated to the results of the vertical component, the elevation angle dependent variations in the IWV are significantly reduced (see Figure 11) by using the Eccosorb, and the two configurations of the installation of the Eccosorb (under the antenna plane only and both under and around) give similar results. The results also show that the radome introduced maximum offset about 0.6 kg/m^2 for the 25° solution, which is slightly larger than 1-σ ($\sim$0.4 kg/m^2) when comparing the data between Sessions D and E (see Figure 12(c)). For the rest of the sessions (see Figure 12(a) and (b)), much less elevation dependence and a small offset (within 0.5 kg/m^2) are caused by the radome. Therefore, the same conclusion as the results from the vertical component can be drawn here. No significant difference ($>$3-σ) in the estimated IWV are evident between the two different configurations of the Eccosorb.

5. CONCLUSIONS

We have shown that the elevation angle dependent effects, i.e. scattering and multipath, have significant influence on the estimates of the vertical component of the relative site position. However, much less elevation angle dependent variations were seen in the horizontal components. The multipath effect can be significantly reduced

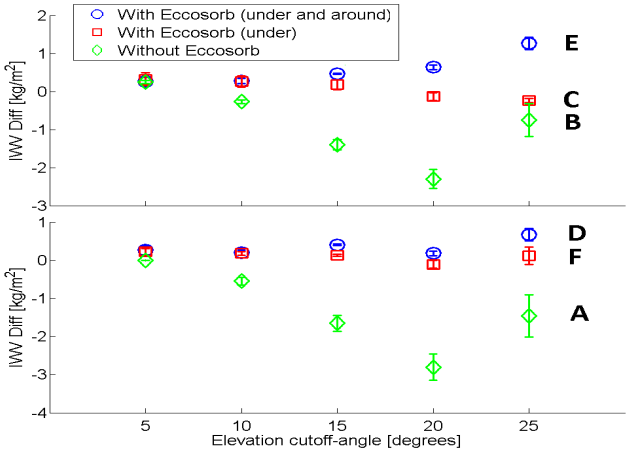

Figure 11. Same as Figure 6 except here for the estimated IWV difference from two GPS stations.

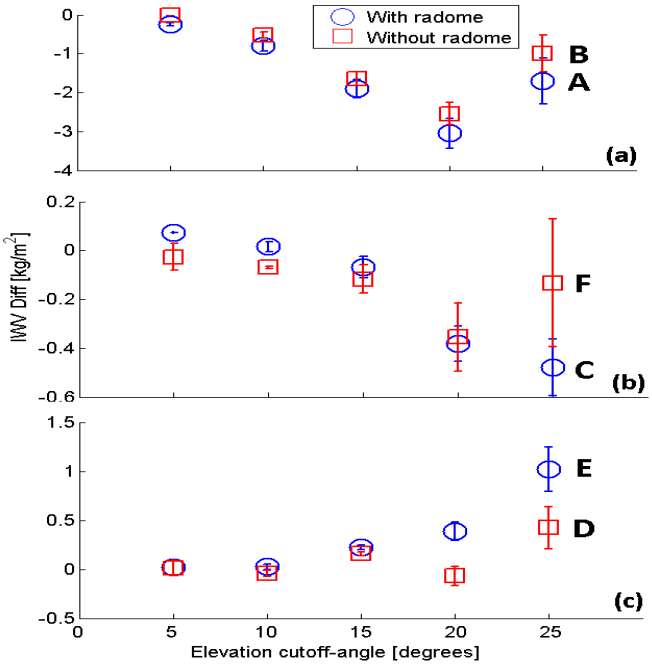

Figure 12. Same as Figure 8 except here for the estimated IWV difference from two GPS stations.

by attaching the microwave absorption material, i.e. Eccosorb, below the antenna. The maximum change in the estimated vertical component of the baseline obtained from the different elevation cutoff angle solutions was decreased approximately from 20 mm to 5 mm when using the Eccosorb. Two configurations of the Eccosorb (put only under or both under and around the antenna) gave similar results proving that the main source of the scattering for the experimental station is the top of the concrete pillar, which is identical to the IGS station (ONSA). Highly correlated to the vertical estimates, the IWV obtained from the two GPS stations also displayed elevation angle dependent variations. The usage of the Ec-

cosorb significantly reduced these variations. No significant deviations (within 0.5 mm) from the different configurations of the Eccosorb with the radome on the antenna. However, different set-up of the Eccosorb without the radome gave clearly different elevation angle dependent variations in the estimated IWV, which can also be seen from the results from the vertical component (see Figure 6(c)). We also see a relatively large difference in the results when the Eccosorb is only put under the antenna plane (see Figure 8(c)). The different results might be due to the non-identical shape of the Eccosorb sheet. When the radome was on the antenna, we reshaped the Eccosorb in order to fit it into the radome (see Figure 1(b)). Hence, repeated experiments for these two situations are necessary to verify this assumption.

We also investigated the influence of the usage of the radome on the GNSS antenna. For 5°, 10°, and 15° elevation cutoff angle solutions, small offsets ($\sim 1-2$ mm) were caused on the estimates of the vertical component of the baseline. The offset went up to around 6 mm for 25° solutions, but with a relatively high uncertainty in 4 mm. No significant deviations (>3-σ uncertainty) in the estimates of the IWV were found. However, these deviations (within 0.5 kg/m^2) may become significant if we are looking for small trends of the IWV in long time series. Therefore, it is recommended that the day of installation or the changing of radome should be carefully recorded.

The multipath effects are normally mixed with the errors caused by the antenna phase center variations. By using the new version of the GIPSY software which included the antenna corrections in advance, the errors introduced by the antenna can be significantly reduced.

REFERENCES

[1] Gradinarsky L.P., 2002, Sesing Atmospheric Water Vapor Using Radio Waves, *Ph.D. theis*, School of Electrical Engineering, Chalmers University of Technology.

[2] Dixon T.H., 1991, An Introduction to the Global Positioning System and some geological applications, *Rev. Geophys.*, 29, 249-276.

[3] Blewitt G., Heflin M., Hurst K., Jefferson D., Webb F., and Zumberge J., 1993, Absolute far-field displacements from the June 28, 1992, Landers earthquake sequence, *Nature*, 361, 340-361.

[4] Elosegui, P., Davis, J.L., Jaldehag, R.T.K., Johansson, J.M., Niell, A.E., and Shapiro, I.I., 1995, Geodesy using the Global Positioning System: the effects of signal scattering on estimates of site position, *J. Geophys. Res.*, 100, B6, 9921-9934.

[5] Jaldehag, R.T.K., Johansson, J.M., Ronnang, B.O., Elosegui, P., Davis, J.L., Shapiro, I.I., and Niell, A.E., 1996, Geodesy using the Swedish permanent GPS network: effects of signal scattering on estimates of relative site positions, *J. Geophys. Res.*, 101, B8, 841-860.

[6] Johansson J.M., Emardson T.R., Jarlemark P.O.J., Gradinarsky L.P., and Elgered G., 1997, The atmospheric influence on the results from the Swedish GPS network, *Physics and Chemistry of the Earth*, 23, 107-112.

[7] Emardson T.R., and Johansson J.M., 2000, The systematic behavior of water vapor estimates using four years of GPS observations, *Trans. IEEE Geosci. Remote Sens.*, 38, 324-329.

[8] Elgered G., and Jarlemark P.O.J., 1998, Ground-based microwave radiometry and long-term observations of atmospheric water vapor, *Radio Sci.*, 33, 707-717.

[9] Webb F.H., and Zumberge J.F., 1993, An introduction to the GIPSY/OASIS-II, *JPL Publ.*.

[10] Zumberge, J.F., Heflin M.B., Jefferson D.C., Watkins M.M., and Webb F.H., 1997, GPS Trends in Precis Terrestrial, Airborne, and Spaceborn Applications, *J. Geophys. Res.*, 102, 5005-5017.

[11] Beutler, G., Mueller I.I., and Neilan R.E., 1996, GPS Trends in Precise Terrestrial, Airborne, and Spaceborn Applications, *Int Assoc Geodesy Symp 115*, 3-13.

[12] Emardson, T.R., and Derks H.J.P., 2000, On the relation between wet delay and the integrated perceptible water vapor in the European atmosphere, *Meteorol. Appl.*, 7, 61-68.

[13] Scherneck, H.-G., and Bos M.S., 2002, Ocean tide and atmospheric loading, *IVS 2002 General Meeting Proc, Int VLBI Service for Geodesy and Astrometry*, 205-214.

[14] Schupler, B.R., and Clark T.A., 1991, How different antennas affect the GPS observable, *GPS World*, 32-36.

[15] Schupler, B.R., Allshouse, R.L., and Clark T.A., 1994, Signal characteristics of GPS user antennas, *Navigation*, 41, 277-295.

[16] Davis, J.L., Herring, I.I, Shapiro, A.E.E., Rogers, and Elgered, G., 1985, Geodesy by radio interfeometry: Effects of atmospheric modeling errors on estimates of baseline length, *Radio. Sci.*, 20, 1593-1607.